Expanded View Figures

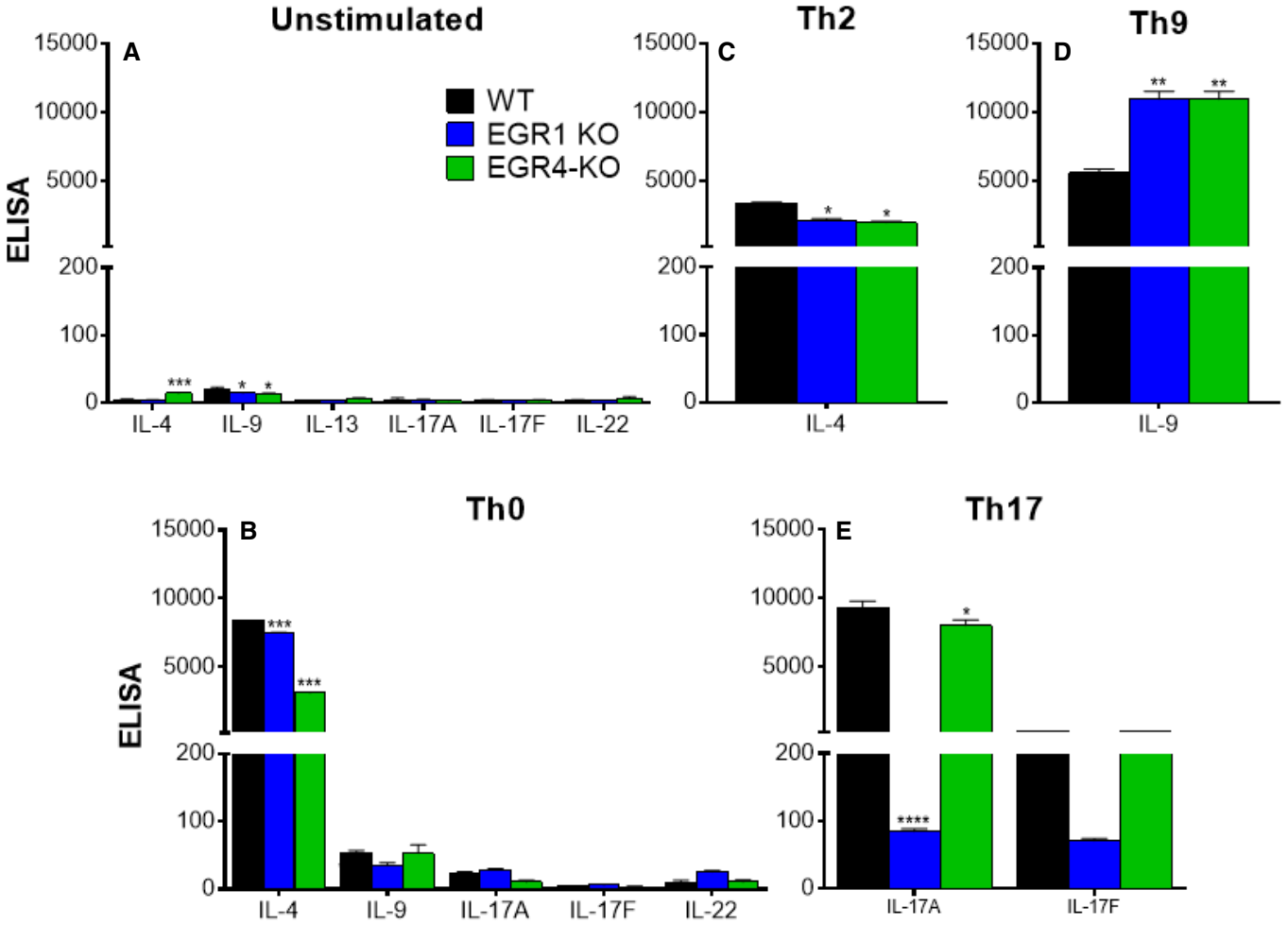

Figure EV1. Cytokine expression patterns in WT, EGR1KO, and EGR4KO CD4$^+$ cells cultured under polarized conditions from Fig 3.

A–E CD4$^+$ T cells were isolated from the spleens of WT, EGR1KO, and EGR4KO mice by cell sorting. Cells were incubated for 5 days without stimulation (A) or under Th0 (B)-, Th2 (C)-, Th9 (D)-, or Th17 (E)-polarizing conditions before analysis of cytokine production by ELISA. Data are presented as mean ± SEM; a minimum of three biological replicates were examined; and each biological replicate includes two technical replicates. Differences in cytokine production were determined by one- or two-way ANOVA as appropriate. Post hoc analysis revealed EGR-dependent differences in cytokine production *$P < 0.05$; **$P < 0.01$; ***$P < 0.001$; ****$P < 0.0001$.

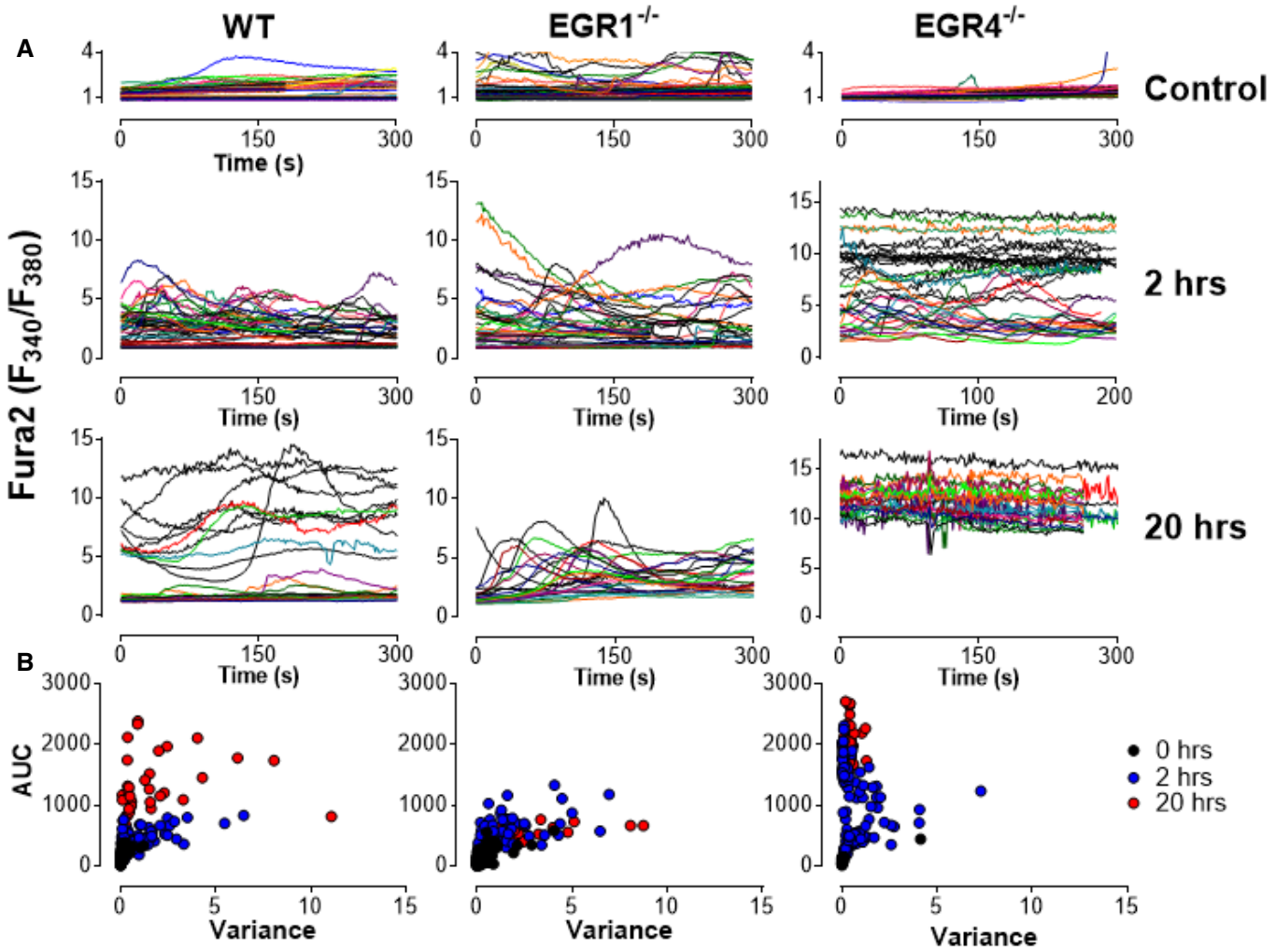

Figure EV2. Activation of CD8$^+$ cells causes sustained Ca^{2+} elevation.

A WT, EGR1KO, and EGR4KO CD8$^+$ T cells were isolated from the spleen by negative selection before plating on poly-lysine (control) or CD3/CD28 and loading with fura-2. Ca^{2+} levels shown are from representative single cells measured from multiple experiments.

B Scatter plots showing area under the curve (AUC) and variance for each cell measured under all conditions.

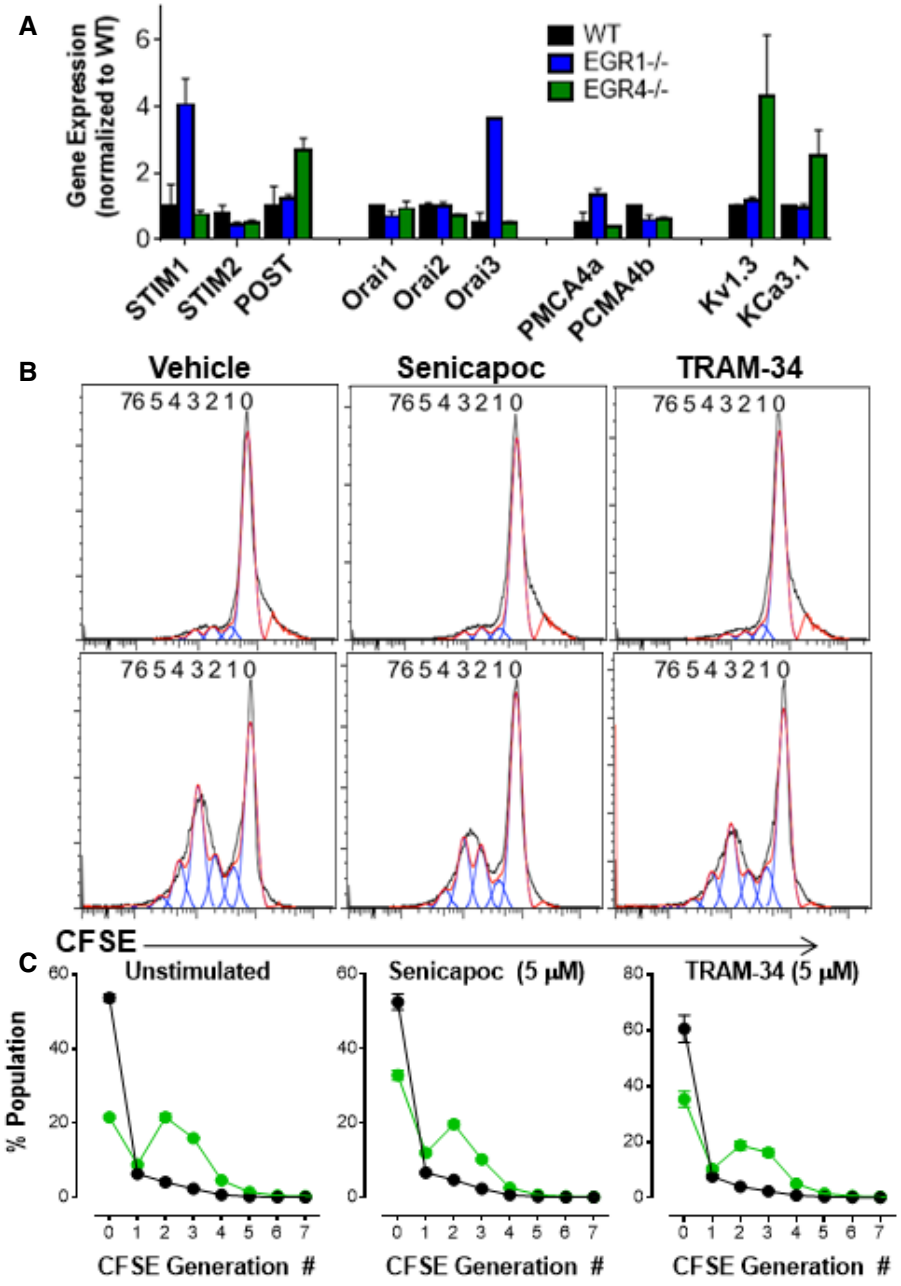

Figure EV3. Inhibition of KCa3.1 has no effect on CD8$^+$ T-cell proliferation.

A–C CD4$^+$ T cells were isolated by negative selection from WT, EGR1$^{-/-}$, or EGR4$^{-/-}$ mice. (A) RNA was collected from freshly isolated cells before probing for STIM1, STIM2, POST, Orai1, Orai2, Orai3, PMCA4a, PMCA4b, Kv1.3, and KCa3.1 expression by qPCR. Data are presented as mean ± SEM; a minimum of three biological replicates were examined; and each biological replicate includes two technical replicates. (B) WT and EGR4$^{-/-}$. CD8$^+$ T cells were isolated from the spleen by cell sorting and stained with CFSE. Cells were incubated with anti-TCRβ antibodies in the presence of vehicle, senicapoc (5 μM), or TRAM-34 (5 μM) for 4 days and then collected for FACS analysis. (C) Generation analysis was completed for all data using FlowJo software. Data are presented as mean ± SEM; a minimum of three biological replicates were examined; and each biological replicate includes two technical replicates.

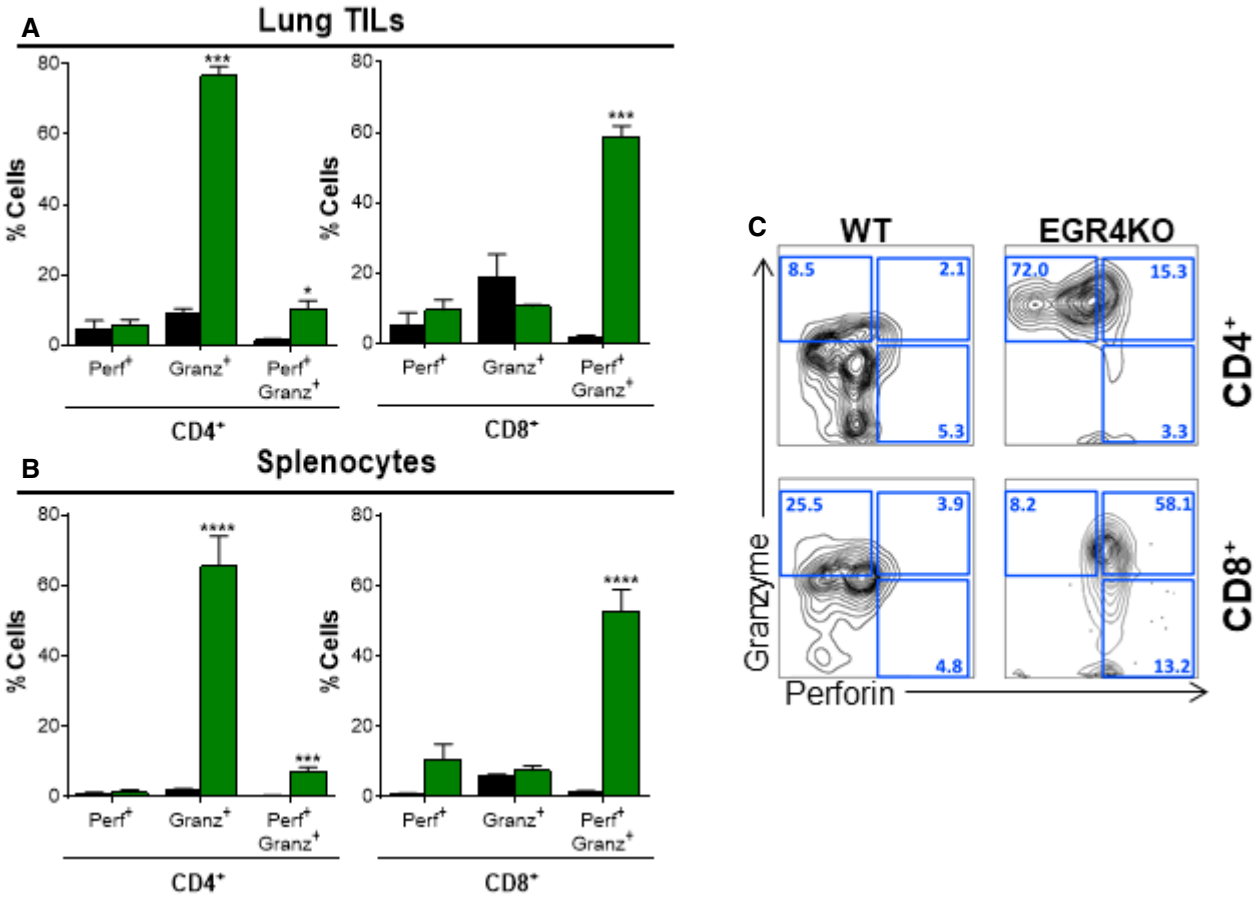

Figure EV4. Increased perforin/granzyme expression in EGR4$^{-/-}$ T cells.

A, B $CD4^+$ and $CD8^+$ cells were stimulated *in vitro* under Th1 conditions in the presence of 25 U/ml IL-2 before intracellular staining for perforin and granzyme B and FACS analysis. Data are mean ± SEM; tumor infiltrates (A) and splenocytes (B) from 10 WT and 4 EGR4$^{-/-}$ mice were examined.

C Representative FACS plots showing cell distributions after staining for perforin and granzyme B. EGR4-mediated differences were determined by paired two-tailed *t*-tests, with significant differences marked by asterisks. *$P < 0.05$; ***$P < 0.001$; ****$P < 0.0001$.

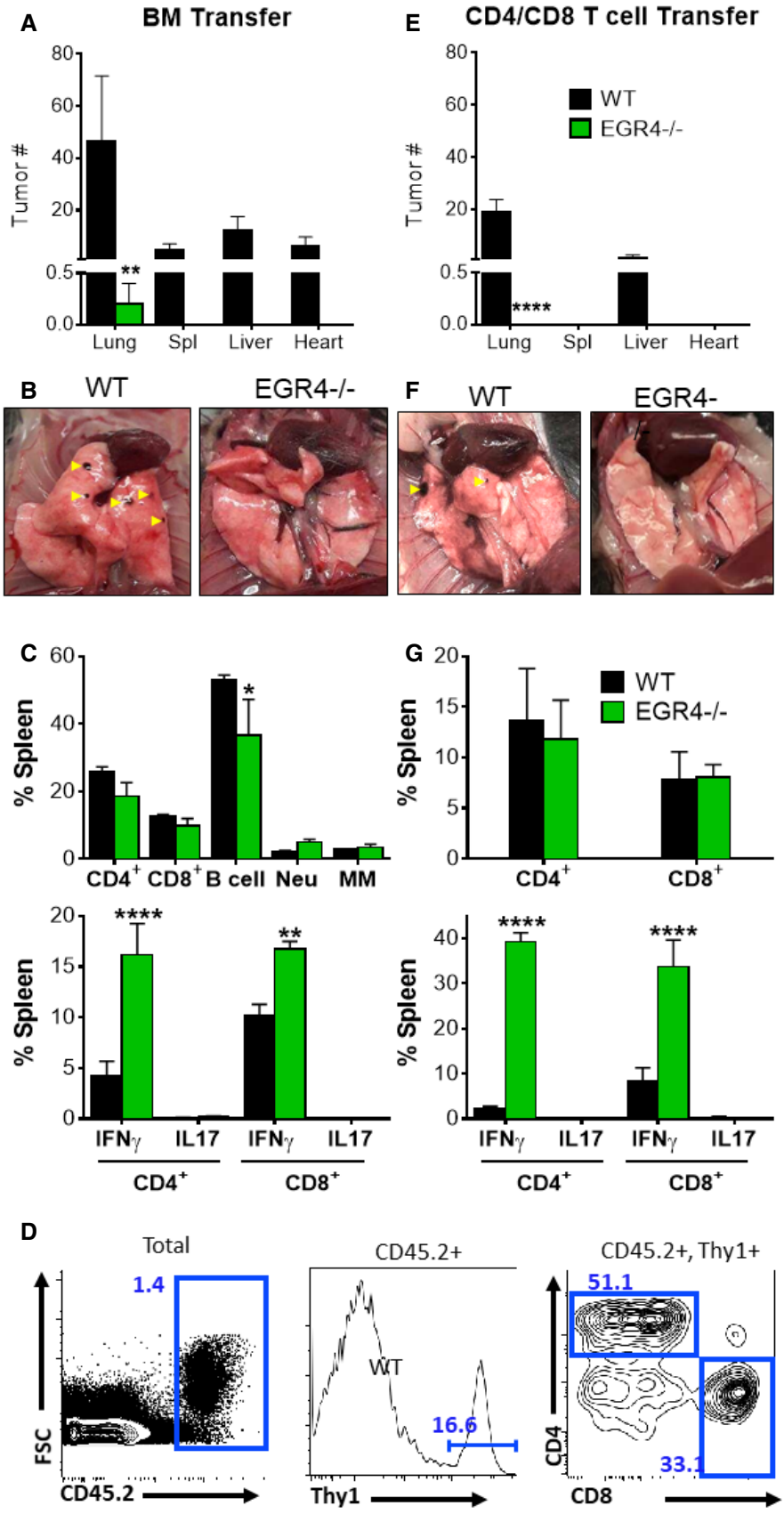

Figure EV5. EGR4KO T cells exhibit enhanced anti-tumor immunity.

A–C Bone marrow (BM) was collected from WT and EGR4$^{-/-}$ mice and reconstituted in RagKO mice.

D–G CD4$^+$ and CD8$^+$ T cells were sorted as depicted (D) before reconstituting in RagKO mice. Mice were sacrificed 21 days after i.v. injection with B6N melanoma cells. Tumor infiltration (black spots marked with yellow arrowheads; B, F) was observed in mice reconstituted with WT bone marrow (A, B) or T cells (E, F), but not after reconstitution with EGR4KO cells.

C, G Since there were no tumors in mice reconstituted with EGR4KO cells, only splenocytes were compared; cytokine expression was determined by flow cytometry after a 5-h stimulation with ionomycin and PMA. Data in panels (A, C, E, and G) are mean ± SEM; data are from RagKO mice containing either bone marrow or T cells from 4 WT or 4 EGR4$^{-/-}$ mice. EGR4-mediated differences were determined by two-way ANOVA, with significant differences marked by asterisks. *$P < 0.05$; **$P < 0.01$; ****$P < 0.0001$ ($N = 4$).